Exploiting Specific Interactions toward Next-Generation Polymeric Drug Transporters

Wieczorek, Sebastian; Krause, Eberhard; Hackbarth, Steffen; Roeder, Beate; Hirsch, Anna K. H.; Boerner, Hans G.

Published in:
Journal of the American Chemical Society

DOI:
10.1021/ja311895z

Publication date:
2013

Supporting Information

Exploiting specific interactions toward next-generation polymeric drug transporters

Journal: J. Am. Chem. Soc.

Corresponding Author: Hans G. Börner*

Other Authors: Sebastian Wieczorek, Eberhard Krause, Steffen Hackbarth, Beate Röder, Anna K. H. Hirsch

* to whom correspondence is to be addressed

Prof. Dr. Hans Börner, Humboldt-Universität zu Berlin, Brook-Taylor-Str. 2, 12489 Berlin, Germany

E-Mail: h.boerner@hu-berlin.de

Phone: +49 (0)30-2093 7348

Fax: +49 (0)30 2093-7500

Materials

N-α-Fmoc protected amino acids Fmoc-Gln(Trt)-OH, Fmoc-Glu(tBu)-OH, Fmoc-Gly-OH, Fmoc-Leu-OH, Fmoc-Lys(Boc)-OH, Fmoc-Met-OH, Fmoc-Phe-OH, Fmoc-Ser(tBu)-OH, as well as 2-(1H-benzotriazole-1-yl)-1,1,3,3-tetramethyluroniumhexafluorophosphate (HBTU), (benzotriazol-1-yloxyl)tripyrrolidinophosphoniumhexa-fluorophosphate (PyBOP) and *N*-methyl-2-pyrrolidone (NMP, 99.9+ %, peptide synthesis grade) were used as received from IRIS Biotech GmbH (Marktredwitz, Germany). TentaGel PAP resin (PEG attached peptide resin, loading: 0.27 mmol/g; Mw = 3200, PDI = 1.04) was obtained from Rapp Polymere GmbH (Tübingen, Germany). Aminomethyl-ChemMatrix® resin (loading: 1.0 mmol/g) was obtained from Sigma Aldrich (St. Louis, MO 63103, USA). *N*,*N*-diisopropylethylamine (DIPEA; Acros, Geel, Belgium, peptide grade), piperidine (Acros, peptide grade), tri-ethylsilane (TES; Alfa Aesar, Karlsruhe, Germany, 98+ %) and guanidine hydrochloride (99.5 %, Roth, Karlsruhe, Germany) have been used as received. Trifluoracetic acid (TFA; Acros, peptide grade) was distilled prior to use. Dichlormethane (DCM, IRIS Biotech GmbH, peptide grade) was distilled from CaH_2 prior to use. Cyanogen bromide (CNBr), ethane dithiol (EDT), Bovin serum albumin fraction V (>96%) were used as received from Aldrich without further purification. *m*-THPC was provided kindly by Professor Mathias O. Senge (School of Chemistry, SFI Tetrapyrrole Laboratory, Trinity College Dublin, Dublin 2, Ireland).

Preparation of the split&mix (One-Bead-One-Compound) peptide library. The peptide library for screening against *m*-THPC was prepared on a Aminomethyl-ChemMatrix® resin (loading 1.0 mmol/g) according to manual single coupling (Fmoc strategy) standard protocols on a 1.5 mmol scale. On this scale, the number of resin beads (approx. 1.4×10^6) is adequate to imply at least one copy of every theoretically possible amino acid sequence (0.8×10^6) in the library. First, a cleavable linker sequence (Gly-Gly-Met) was synthesized on the resin by addition of the corresponding Fmoc-AA-OH (5 eq.) with PyBOP (5 eq.) and DIPEA (10 eq.) in NMP and gentle shaking overnight at room temperature. The resin was washed, acetylated with acetic anhydride (10 %) and DIPEA (10 %) in NMP (2 × 10 min.) and washed again. Fmoc deprotection was achieved by treatment with piperidine (20 %) in NMP (3 × 10 min.), followed by a

final washing step and coupling of the next amino acid. The variable peptide segment was synthesized manually by splitting the resin in seven aliquots containing equal amounts of resin, followed by reacting with 5 eq. of a different Fmoc protected amino acid (Gly, Leu, Ser, Phe, Glu, Gln, Lys) with PyBOP (5 eq.) and DIPEA (10 eq.) in NMP overnight for each aliquot (**Figure S1(A)**). Subsequently, all resin aliquots were mixed for washing, acetylation and Fmoc deprotection (see above). This cycle of splitting and mixing was repeated, until the desired library size (7^7 different peptides) was accomplished. Finally, the resin was treated with a mixture of 94 % TFA, 2.5 % TES, 2.5 % EDT, 1 % deionized water to remove side chain protecting groups, followed by intensive washing with DCM and drying of the resin *in vacuo*.

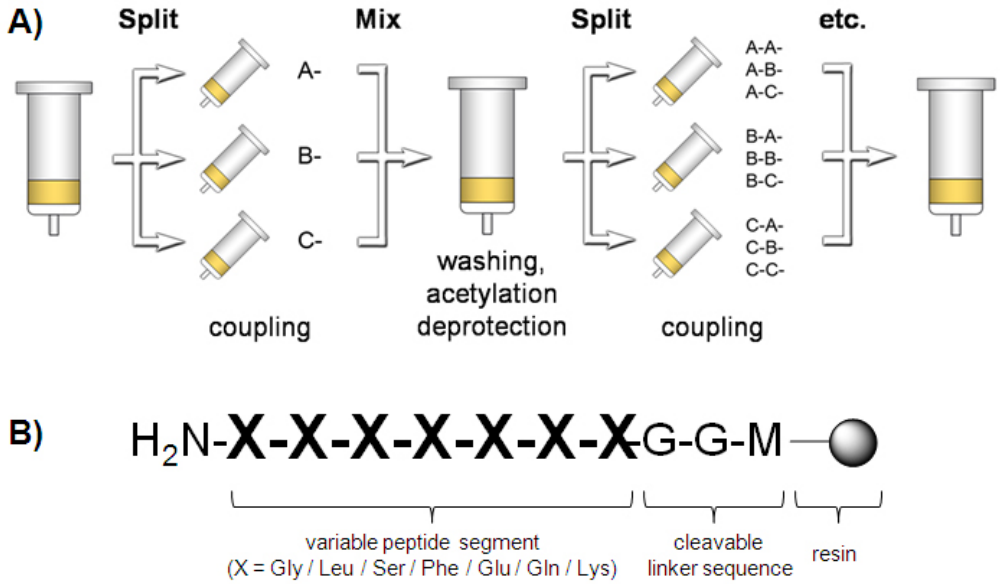

Fig. S1. (A) Schematic representation of the split&mix peptide library synthesis procedure. (B) Design of the immobilized peptides used for screening against *m*-THPC.

Peptide library screening against *m*-THPC. The resin bound peptide library was incubated with crystalline *m*-THPC (1 mg/mL) in a mixture of deionized water and EtOH (9:1 v/v) and stirred for 72 h (RT) in a glass vial. The resin was washed with EtOH and filtered several times, followed by storage in an EtOH/water mixture (1:1 v/v) overnight to remove any non-specifically bound *m*-THPC. Enrichment of *m*-THPC on beads carrying a peptide sequence with high affinity to non-covalent binding of *m*-THPC was followed via fluorescence microscopy (**Figure S2**). Control experiments containing solid-phase resin without immobilized peptides incubated with *m*-THPC and library beads

without *m*-THPC incubation were performed as well (**Figure S3**). A *Zeiss Axio* fluorescence microscope (Carl Zeiss MicroImaging GmbH, 07745 Jena, Germany) including an *Axio Observer.A1* platform with a *HAL 100* transmission light source, an *AxioCam MRm* and a *HXP 120C* mercury lamp (Leistungselektronik Jena GmbH, D-07747 Jena, Germany) was used. Intrinsic fluorescence of *m*-THPC was excited and recorded via a *Zeiss filter set 50* (Cy5) and pictures were recorded and evaluated with the *Zeiss AxioVision* software package.

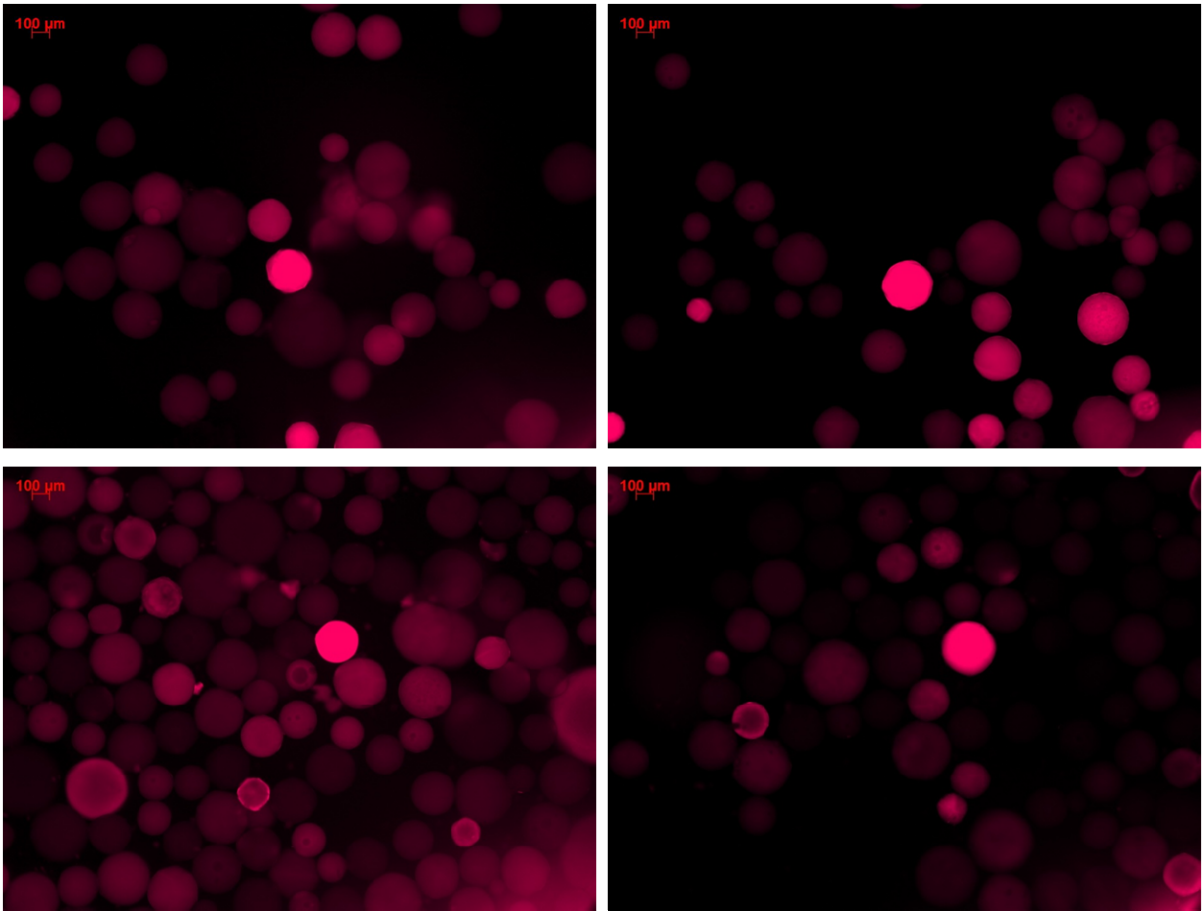

Fig. S2. Fluorescence microscopy images of resin-bound split&mix peptide library. Examples of picked positive hits showing enrichment of *m*-THPC on certain resin beads prior to isolation and cleavage.

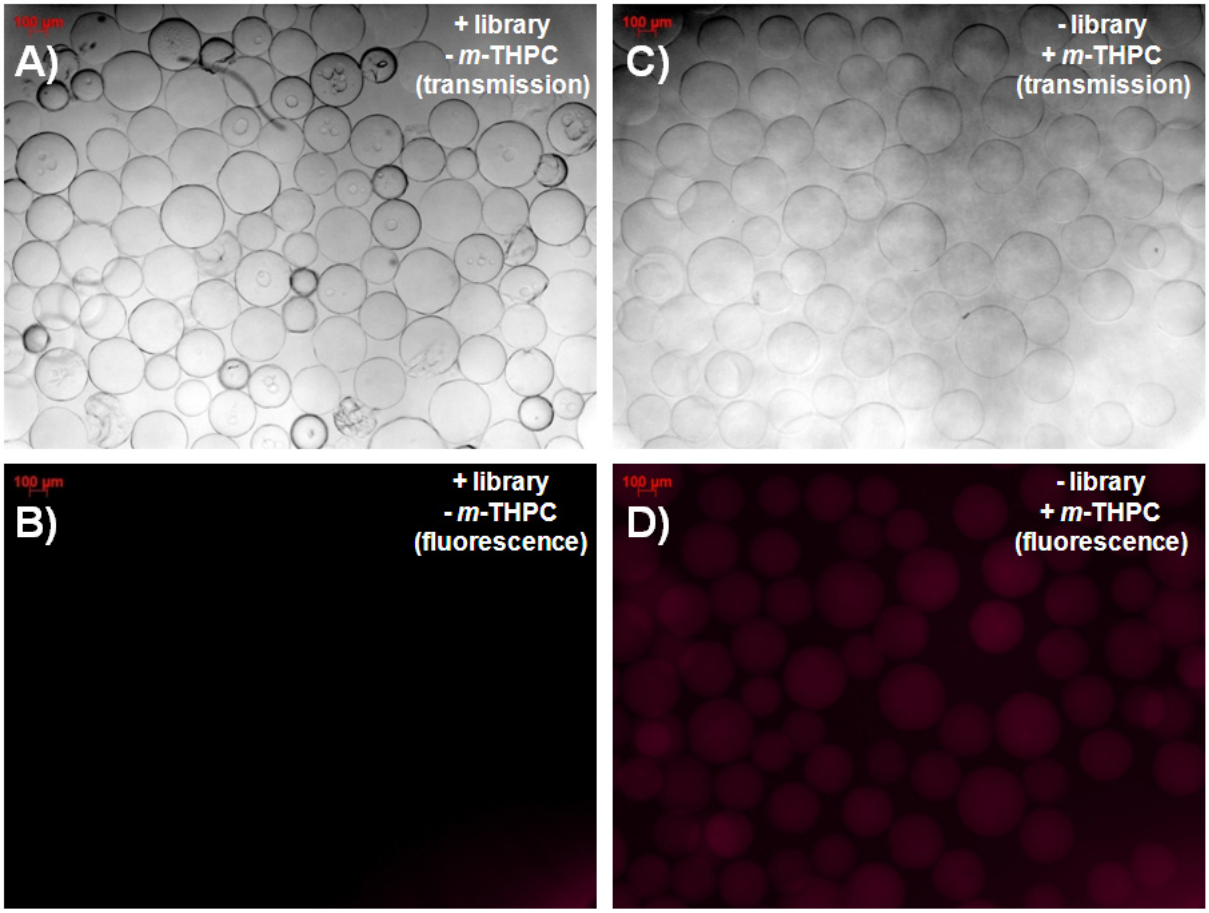

Fig. S3. Fluorescence microscopy images of control experiments. Resin bound split&mix (One-Bead-One-Compound) peptide library in (A) transmission and (B) fluorescence mode. Solid-phase resin without immobilized peptides incubated with *m*-THPC in (C) transmission and (D) fluorescence mode.

Separation of positive hits, peptide cleavage and acetylation. Fluorescing beads were removed from suspension and transferred individually into 0.2 mL PCR tubes. Immobilized peptides were cleaved from the solid support via treatment with 20 µL CNBr (20 mg/mL) dissolved in 0.1 M HCl overnight at room temperature. The solutions were freeze-dried and residues were acetylated to distinguish Gln and Lys in MS analysis. To do so, residues were dissolved in acetone (40 µL), Ac_2O / AcOH (10 µL, 1:1 v/v) were added, and the mixtures were shaken at room temperature for 1 h. Afterwards, 20 µL acetonitrile / water (1:1 v/v) with 0.1 % TFA were added, acetone was removed with an argon stream and the solutions were freeze-dried again. Residues were dissolved in acetonitrile / water (1:1 v/v) + 0.1 % TFA and subjected to MALDI-ToF-MS/MS analysis.

Peptide sequencing by MALDI tandem mass spectrometry. Sequencing was performed with an *5800 MALDI ToF/ToF* system (AB SIEX, Framingham, MA, USA) equipped with an Neodymium-doped yttrium lithium fluoride (Nd:YLF) laser (349 nm, 1000 Hz working frequency). 1 µL of peptide solution was spotted on the MALDI plate together with 1 µL alpha-cyano-4-hydroxycinnamic acid (5 mg/mL) matrix in acetonitrile / water (0.65 : 0.35, v/v) + 0.3 % TFA and dried by exposure to air. MS spectra were gained in positive ion reflectron mode as an average of 4,000 laser shots. Precursor ions were selected after MS measurement according to fixed criteria (5 most intensive peaks, S/N > 20). Fragmentation spectra were recorded using 5,000 laser shots. Precursor mass window was set to 200 (FWHM), collision energy was 1 keV and air was used as collision gas. *GPS Explorer* (Version 3.6, Applied Biosystems) was used for data processing and transfer to a *MASCOT* Server (Version 2.2, Matrix Science Ltd., London, UK) for database search from a custom made file containing all theoretically possible peptide sequences (823,543 different sequences). Results of MS/MS sequencing are summarized in **Table S1** and **Figure S4**.

Table S1. Peptide sequences obtained by MS/MS analysis of separated positive hits from the split&mix peptide library (MS/MS hits with equal ion score are listed in the same row, Pos = position in the peptide sequence).

	NH2-[Pos1]	[Pos2]	[Pos3]	[Pos4]	[Pos5]	[Pos6]	[Pos7]	Ion Score
1	F	Q	E	L	F	G	F	82
2	F	F	L	F	F	S	F	77
3	F	F	Q	Q	F	Q	E	72
4	F	F	G	Q	E	F	F	57
5	S	L	K	L	Q	F	S	57
6	L	L	E	L	F	G	F	53
7	F	F	E	L	E	S	L	36
8	F	F	E	Q	F	Q	S	36
	F	E	F	Q	F	Q	S	36
9	S	F	F	E	F	S	L	34
10	F	F	E	S	F	Q	S	33
	F	E	F	S	F	Q	S	33
11	F	E	L	F	G	E	L	33
12	L	F	L	L	L	L	L	26
13	L	Q	Q	S	F	F	F	23
14	F	F	E	E	E	K	S	21
15	G	F	L	F	G	G	L	21
16	L	Q	K	Q	F	Q	S	20
17	F	E	G	L	G	F	L	19
18	K	F	E	L	L	Q	S	18
19	S	E	K	E	Q	F	L	18
20	Q	F	F	L	S	F	F	17
	Q	F	F	L	F	S	F	17
	Q	F	F	L	F	F	S	17
21	Q	Q	Q	Q	F	Q	K	17
22	K	L	G	F	Q	F	Q	16
23	L	L	L	F	Q	L	L	16
24	F	F	E	Q	F	F	S	14
25	G	L	L	E	F	F	F	13
26	Q	F	F	L	Q	K	F	11
27	Q	F	L	F	G	Q	L	9
28	F	S	F	F	S	G	Q	9
29	S	L	F	G	F	F	E	9
30	F	L	Q	K	F	F	E	9
31	F	F	L	F	G	G	S	8
32	S	K	L	E	S	Q	L	8
33	L	Q	Q	F	F	G	S	7
34	F	Q	F	S	S	Q	S	7
35	Q	G	F	G	Q	E	Q	7
36	S	F	G	F	F	F	E	7
37	L	F	L	F	F	E	Q	6
38	G	G	S	L	E	E	E	6
39	G	G	G	F	F	E	K	6
40	G	L	Q	F	L	L	Q	6
41	K	F	F	Q	F	S	Q	5

Color code: Aromatic/hydrophobic (yellow); polar (green); aliphatic/hydrophobic (black); cationic/polar (blue); anionic/polar (red)

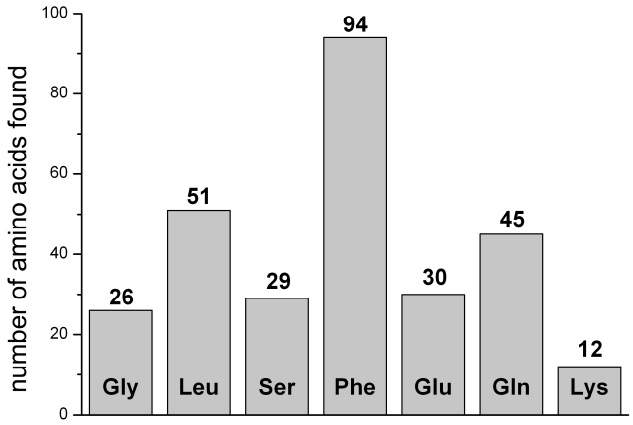

Fig. S4. Amino acid composition found by MALDI-ToF-MS/MS analysis for screening of *m*-THPC against the split&mix (One-Bead-One-Compound) peptide library.

Peptide-PEO conjugate (P I – P III) synthesis. Peptide-PEO conjugates were obtained by automated solid-phase peptide synthesis on an *ABI 433a* peptide synthesizer (Applied Biosystems, Foster City, CA 94404, USA) following standard *ABI-Fastmoc* protocol (single coupling) with NMP as solvent. As solid support, Tentagel-PAP resin (Rapp Polymere GmbH, D-72072 Tübingen, Germany) with a loading of 0.27 mmol/g was used. The resin carries an α-hydroxy-ω-amino-functionalized PEO (approx. 3 kDa), which is coupled to the resin via an acid-labile benzyl ether linker molecule. After stepwise polypeptide assembly via HBTU/NMP/piperidine protocol, conjugates were cleaved from the solid support by treatment with a mixture of 95 % TFA, 4 % TES and 1 % water at room temperature for 3 h. The resin was filtered, washed with TFA and the collected supernatants were concentrated in vacuo. Afterwards, peptide conjugates were precipitated in cold diethyl ether, centrifuged (20 min., 9000 rpm) and the supernatants were removed by decantation. Precipitates were dried in vacuo, dissolved in deionized water with 1 % guanidine hydrochloride and pH was adjusted to neutrality. Subsequent, peptide conjugates were dialyzed against deionized water (500-1000 Da MWCO, regenerated cellulose), followed by freeze-drying of conjugate solutions.

Peptide conjugate characterization: Peptide conjugates were characterized by MALDI-MS measured with a *5800 MALDI ToF/ToF* system (AB SIEX, Framingham, MA, USA) as described before, but in MS mode without fragmentation of the peptide sequence. ^{1}H nuclear magnetic resonance spectra (^{1}H-NMR) were recorded on a Bruker AV 500 spectrometer at 500 MHz in TFA-d_1 at room temperature. Fourier transform infrared spectroscopy (ATR-FT-IR) was carried out on a Jasco FT/IR-4200 Fourier Transform Infrared Spectrometer (Golden gate).

Analysis of P I:

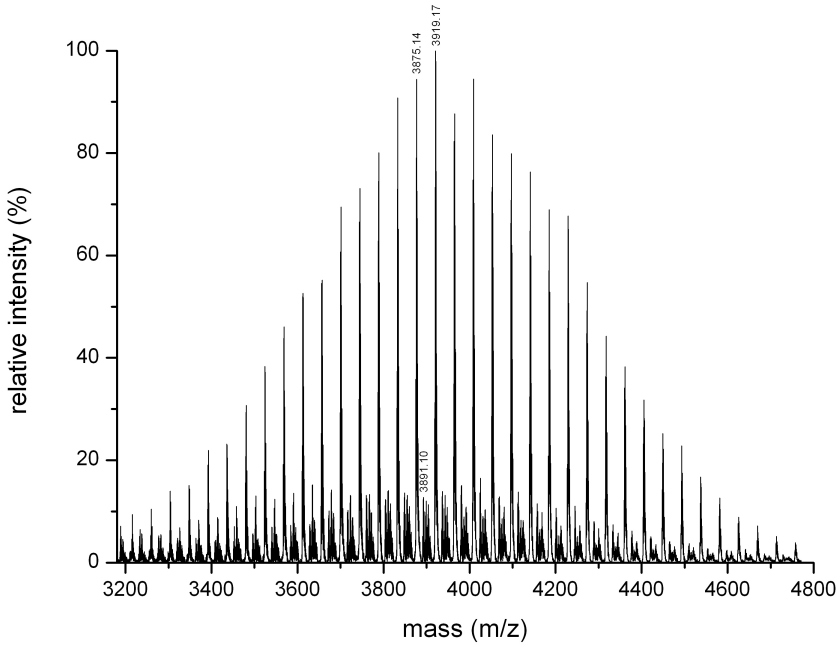

Fig. S5. MALDI-ToF-MS of P I.

$M_{peak}[M+Na]^+$ = 3919.17 (m/z) $M_{calc}[M+Na]^+$ = 3919.43 Da

$M_{peak}[M+K]^+$ = 3891.10 (m/z) $M_{calc}[M+K]^+$ = 3890.50 Da

Δm = 44.03 Da (EO repeat unit).

$M = M_{peptide} + M_{PEO(66)} + M_{Na}$ = 3919.43 Da. The signal can be assigned within ± 0.3 Da accuracy.

^{1}H NMR (500 MHz, TFA-d, δ in ppm): 7.23-6.94 (m, 20H, CH^{Ar} Phe), 4.86-4.59 (m, 7H, $C^{\alpha}H$), 4.00-3.54 (m, 308H, PEO), 3.19-2.46 (m, 18H, CH_2 Phe, $C^{\beta+\gamma}H_2$ Gln, $C^{\delta}H_2$ Glu), 2.12-1.88 (m, 4H, $C^{\beta+\gamma}H_2$ Glu). The ratio of peptide vs. EO was determined by comparison of integral intensities of 20H from CH^{Ar} Phe at 7.23-6.94 ppm and 308H of PEO at 4.00-3.54 ppm to correspond to a ratio of 1:77.

FT-IR (υ(cm-1)): 3272 (vw), 2885 (m), 1659 (w), 1636 (w), 1540 (w), 1466 (w), 1407 (vw), 1343 (m), 1281 (m), 1240 (w), 1146 (m), 1109 (vs, PEO), 1064 (m), 960 (m), 843 (m), 748 (vw), 688 (vw).

Analysis of P II:

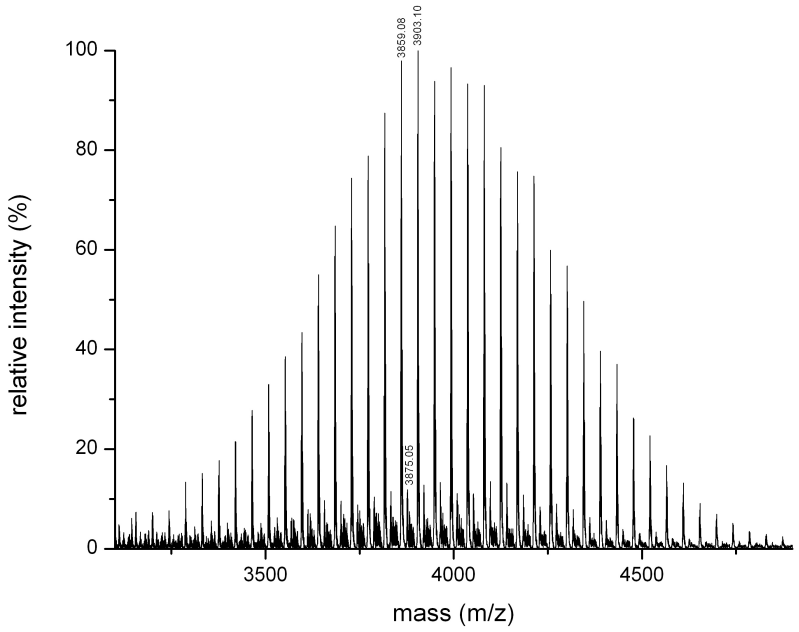

Fig. S6. MALDI-ToF-MS of P II.

$M_{peak}[M+Na]^+$ = 3903.10 (m/z) $M_{calc}[M+Na]^+$ = 3903.44 Da

$M_{peak}[M+K]^+$ = 3875.05 (m/z) $M_{calc}[M+K]^+$ = 3875.52 Da

Δm = 44.02 Da (EO repeat unit).

$M = M_{peptide} + M_{PEO(66)} + M_{Na}$ = 3903.44 Da. The signal can be assigned within ± 0.3 Da accuracy.

^{1}H NMR (500 MHz, TFA-d, δ in ppm): 7.25-6.91 (m, 20H, CH^{Ar} Phe), 4.74-4.39 (m, 7H, $C^{\alpha}H$), 3.99-3.55 (m, 288H, PEO), 3.05-2.50 (m, 16H, CH_2 Phe, $C^{\beta+\gamma}H_2$ Gln), 1.51-1.42 (m, 4H, $C^{\beta+\gamma}H_2$ Leu), 0.93-0.85 (m, 6H, CH_3 Leu). The ratio of peptide vs. EO was determined by comparison of integral intensities of 20H from CH^{Ar} Phe at 7.25-6.91 ppm and 288H of PEO at 3.99-3.55 ppm to correspond to a ratio of 1:72.

FT-IR (υ(cm-1)): 3274 (m), 2886 (s), 1667 (m), 1633 (s), 1549 (m), 1466 (m), 1407 (vw), 1344 (m), 1280 (s), 1240 (m), 1201 (w), 1145 (s), 1112 (vs, PEO), 1065 (m), 960 (m), 843 (m), 744 (vw), 698 (vw).

Analysis of PIII:

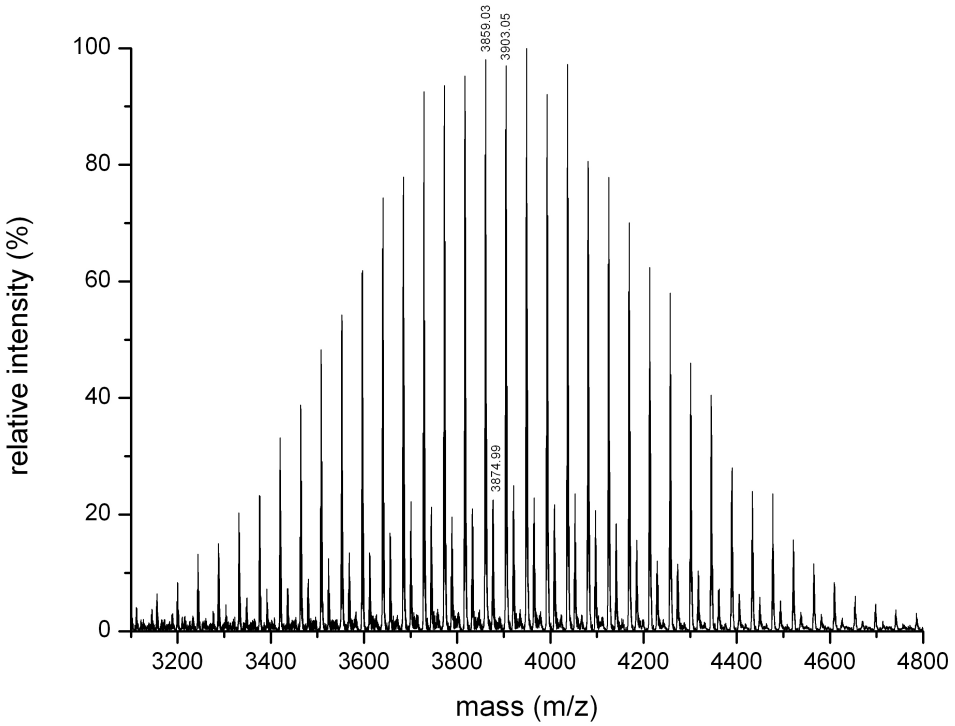

Fig. S7. MALDI-ToF-MS of P III.

$M_{peak}[M+Na]^+$ = m/z 3859.03 (m/z) $M_{calc}[M+Na]^+$ = 3859.39 Da

$M_{peak}[M+K]^+$ = m/z 3874.99 (m/z) $M_{calc}[M+K]^+$ = 3875.50 Da

Δm = 44.02 Da (EO repeat unit).

$M = M_{peptide} + M_{PEO(66)} + M_{Na}$ = 3859.39 Da. The signal can be assigned within ± 0.4 Da accuracy.

^{1}H NMR (500 MHz, TFA-d, δ in ppm): 7.30-7.02 (m, 15H, CH^{Ar} Phe), 4.67-4.54 (m, 7H, $C^{\alpha}H$), 4.15 (dd, *J* = 54.2, 9.3 Hz, 2H, $C^{\beta}H_2$ Ser), 3.99-3.61 (m, 272H, PEO), 3.31-3.00 (m, 8H, CH_2 Phe, $C^{\delta}H_2$ Glu), 2.64-2.50 (m, 8H, $C^{\beta+\gamma}H_2$ Gln), 2.16-1.95 (m, 4H, $C^{\beta+\gamma}H_2$ Glu).

The ratio of peptide vs. EO was determined by comparison of integral intensities of 15H from CH^{Ar} Phe at 7.30-7.02 ppm and 272H of PEO at 3.99-3.61 ppm to correspond to a ratio of 1:68.

FT-IR (υ(cm-1)): 3285 (w), 2879 (m), 1696 (m), 1632 (s), 1519 (m), 1467 (m), 1412 (vw), 1359 (m), 1342 (m), 1280 (s), 1241 (m), 1200 (w), 1145 (s), 1098 (vs, PEO), 1060 (m), 961 (m), 842 (m), 745 (vw), 696 (vw).

Modeling and estimation of the binding energy. The three-dimensional structures of the peptides P I, P II and P III were generated using the software CORINA,[1] and manually docked onto the structure of *m*-THPC. The energy of the peptide–*m*-THPC complexes was minimized using the MAB force field as implemented in the computer program MOLOC,[2] while keeping the coordinates of *m*-THPC fixed. During the modeling, the PEO chain was not taken into account.

One main pose was identified for peptides P I and P II. According to the modeling, favorable interactions of the side chains of the aromatic amino acids with the aromatic system of *m*-THPC are established: face-to-face, offset face-to-face and edge-to-face π-π interactions with amino acids Phe2 and Phe3, Phe5 and Phe6, respectively. The side chain of Glu4 in P I is involved in a strong hydrogen bond with one phenolic hydroxyl group of the *m*-THPC ($d(O^{\cdots}O)$ = 3.02 Å), ensuring that the peptide-*m*-THPC complex is stabilized by several other non-covalent interactions. Likewise, the side chain of Leu4 in P II is involved in a favorable hydrophobic interaction with the aromatic system of *m*-THPC. In addition, the hydroxyl groups of the *m*-THPC are also engaged in some other hydrogen bonds. Both the side chain of Gln1 ($d(O^{\cdots}O)$ = 2.89 Å) and the backbone of Phe5 ($d(O^{\cdots}O)$ = 3.02 Å) in P II, are hydrogen bond acceptors. In P I, Gln1 ($d(O^{\cdots}O)$ = 2.70 Å) and Phe5 ($d(O^{\cdots}O)$ = 2.95 Å) are also involved in hydrogen bonds with the hydroxyl groups of *m*-THPC.

A different pose was identified for peptide P III. The whole structure of the peptide is less stretched and more folded, with the amino acids bearing polar and charged side chains being more exposed to

the solvent. The residues Phe1, Phe2 and Phe5 are involved in edge-to-face and offset face-to-face π-π interaction and contribute to the stabilization of the peptide–mTHPC complex. One strong hydrogen bond is formed between one hydroxyl group of *m*-THPC and the first oxygen atom of the PEG linker (d(O···O) = 2.82 Å) and two weaker hydrogen bonds involve the backbone of Phe2 (d(O···O) = 2.86 Å) and the side chain of Gln4 (d(O···O) = 3.16 Å).

Using the docking program LeadIT, the modeled poses were ranked according to their free energies of binding as calculated by the HYDE scoring function as implemented in LeadIT.[3] The HYDE scoring function was used to evaluate the peptide–m-THPC complexes. To do so, the structures were protonated with FCONV,[4] and the calculated binding energies are reported in Table S2.

Images in Figure 4 were generated with Pymol.

Table S2. Structures and HYDE scores of peptides **P I**, **P II** and **P III**.

Compound	Peptide	HYDE score /kJmol^{-1}
P I	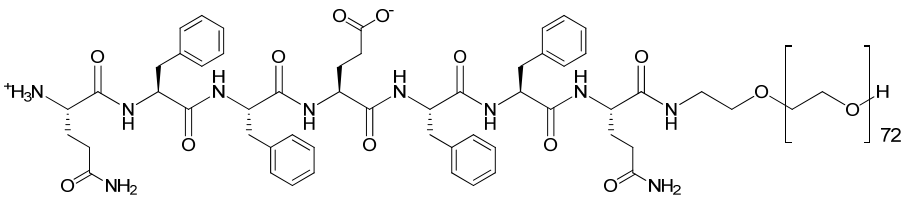	−23
P II	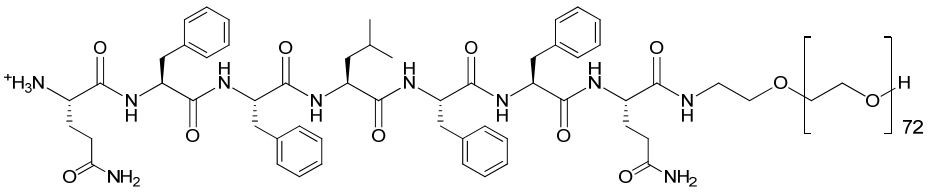	−29
P III	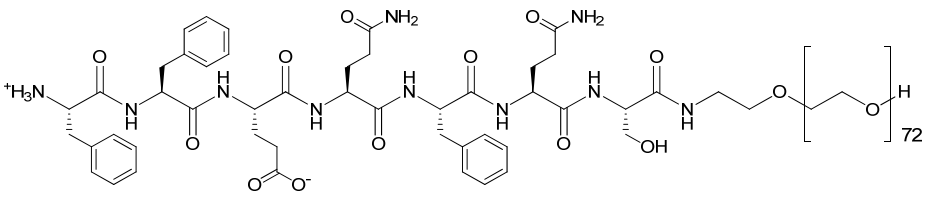	−23

Solubilization of *m*-THPC by peptide-PEO conjugates (P I – P III) and Pluronic® F68 (BASF). *m*-THPC was dissolved in EtOH (1 mg/mL) and 1 mL (1.47 µmol *m*-THPC) of the solution was added to solutions of each transporter (1.47 µmol) in deionized water (1 mL, pH 7). The resulting mixtures were shaken at room temperature for 1 h, followed by freezing in lq. N_2 and freeze drying *in vacuo*. Residues were dissolved in deionized water (1 mL, pH 7) and solutions were centrifuged (30 min., 10000 rpm) to remove not solubilized *m*-THPC. UV-Vis absorption spectra of each supernatant were recorded on a *Shimadzu UV-2501 PC* spectrometer (Shimadzu Corp., 604-8511 Kyoto, Japan) using quartz glass cuvettes (1 mL, 10 mm path) against a reference containing water (**Figure S8**). Concentration of solubilized *m*-THPC by each carrier was calculated via comparison of the absorption maximum at 655 nm with a calibration curve of the free drug in EtOH (0.0001, 0.0005, 0.001, 0.005, 0.01 mg/mL). To do so, 100 µL of each *m*-THPC carrier complex in water was added to 900 µL of EtOH and absorption spectra of each solution (diluted 1:100 in EtOH) were recorded. Maximum payload capacity of each carrier is summarized in **Table S3**.

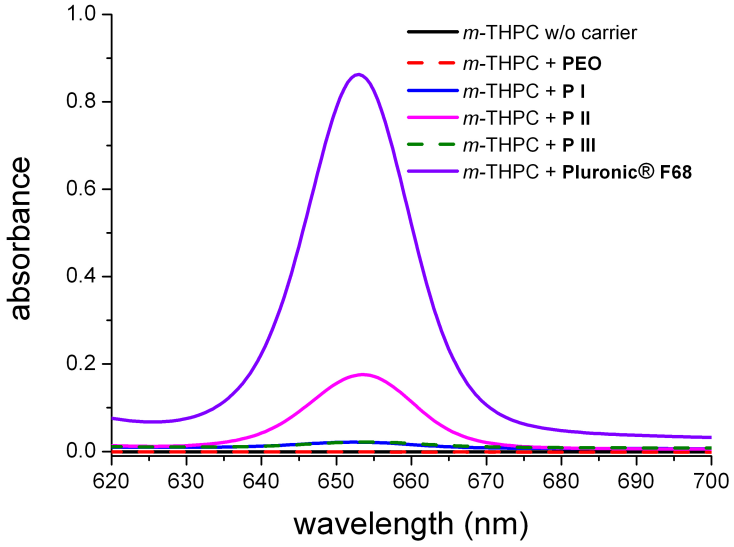

Fig. S8. UV-Vis absorption spectra (Zoom-in) of *m*-THPC solubilized by different carrier molecules in deionized water (1:100 dilutions, pH 7). Carrier concentration was fixed (1.47 mM) and carriers were saturated with *m*-THPC by freeze drying. Spectra represent the maximum payload capacity of each carrier system.

Table S3. Concentration of solubilized *m*-THPC by each carrier system achieved by incubation and freeze-drying of carrier and drug in water / EtOH and resuspension in water (n.d. = not detectable).

	water w/o carrier	**PEO-2000**	**P I**	**P II**	**P III**	**Pluronic® F68**
Carrier conc. (mM)	-	1.47	1.47	1.47	1.47	1.47
Initial *m*-THPC conc. (mM)	1.47	1.47	1.47	1.47	1.47	2.94
Solubilized *m*-THPC conc. (mM)	n.d.	n.d.	0.09	0.45	0.04	2.15
m-THPC / carrier ratio	-	-	1 : 16	1 : 3.2	1 : 37	1 : 0.7

Fluorescence emission. Steady-state fluorescence emission spectra were recorded on a *Cary Eclipse* fluorescence spectrophotometer (Varian/Agilent Technologies, Santa Clara, California, USA) in 10 mm polystyrene sample cells. None of the tested carrier system (P I-P III, Pluronic® F68) showed significant fluorescence emission upon saturation with their individual maximum payload of *m*-THPC (data not shown). Fluorescence emission triggering of carriers with maximum *m*-THPC loading was measured via incubation with BSA. To do so, each stock solution of *m*-THPC (2 µM) and carrier (variable concentration depending on maximum payload of each system) complexes in deionized water (1 mL, pH 7) was mixed with a solution of BSA (1 mL, 100 µM) in deionized water (pH 7). Immediately, fluorescence-emission spectra (em.: 620–700 nm, exc.: 417 nm) were recorded with a 5 minute delay for a period of 18 h. Fluorescence emission intensity at 653 nm was plotted against time (**Figure 5(B)**).

To prove that increasing fluorescence emission is a matter of BSA addition, *m*-THPC loaded P II was measured over time without protein incubation (data not shown). No fluorescence emission triggering was observed without the addition of BSA.

In contrast to carriers saturated with *m*-THPC, P II and Pluronic® F68 loaded with low amount of *m*-THPC (1:50 mol/mol) showed strong fluorescence emission at 653 nm upon excitation (data not shown). This indicates that quenching of fluorescence emission and singlet oxygen generation can be attributed to a very high local concentration of drug molecules in saturated drug / carries aggregates.

Dynamic light scattering. Dynamic light scattering (DLS) experiments were carried out on a spectrometer consisting of an argon ion laser (λ = 488 / 633 nm, intensity: 30-600 mW; Coherent Innova 300), a self-constructed goniometer, a single-photon detector (ALV SO-SIPD) and a multiple-tau digital correlator (ALV-5000/FAST). DLS autocorrelation functions were measured at a conjugate concentration of 0.37 µM and a scattering angle of 90°. Autocorrelation functions were evaluated with the program FASTORT.EXE[5] to obtain diffusion coefficients, which were transformed into hydrodynamic radii via the Stokes–Einstein equation (**Table S4**). For P I and P III without *m*-THPC, no structures >7 nm (detection limit of the scattering setup) were detected.

Table S4. Hydrodynamic radii obtained by dynamic light scattering measurements of conjugate transporters P I–P III not loaded (top) und loaded (bottom) with *m*-THPC.

	P I	**P II**	**P III**
- *m*-THPC	n.d.	R_h = 37.2 nm	n.d.
+ *m*-THPC	R_h = 63.8 nm	R_h = 164.8 nm	R_h = 74.8 nm

Singlet oxygen generation. Time-resolved singlet oxygen [$^1O_2$] luminescence around 1270 nm was detected using a recently described setup[6] that is based on the NIR photomultiplier H10330 from Hamamatsu. Illumination is performed by LEDs with a central wavelength at 425 nm driven by a custom-made controller with pulses at a repetition rate of about 12 kHz and with a nearly rectangular temporal intensity profile of 160 ns duration. Wavelength discrimination of the emitted light is done by a silicon edge filter and a band pass interference filter with central wavelength at 1270 nm and 30 nm FWHM. Nevertheless, a short time artifact is present in each measurement. It has several reasons (e.g. scattering, luminescence, hot spots) and can never be completely eliminated. Therefore for the fitting the first 1 µs is omitted.

In a homogeneous environment the measured $^1O_2$ luminescence intensity I(t) can normally be described by a double exponential function[7-11]:

$$I(t) = \left(C \cdot n_T \cdot \Phi_\Delta\right) \cdot \frac{\tau_T^{-1}}{\tau_T^{-1} - \tau_O^{-1}} \left(\exp[-t/\tau_O] - \exp[-t/\tau_T]\right)$$

where τ_T is the photosensitizer triplet and τ_O is the $^1O_2$ decay time. The amplitude that was determined consists of n_T - the number of molecules initially in the triplet state after excitation, Φ_Δ - the quantum yield of $^1O_2$ generation and C - a constant factor that represents the detection efficiency of the setup.

It has been shown,[6,11] that for membrane-located photosensitizers an additional signal component appears due to a higher radiative rate constant of $^1O_2$ at the generation site before it diffuses into the surrounding water. For times larger than 1 µs after the pulse, a first approximation of this additional signal component yields an additional mono exponential decay determined by the photosensitizer triplet decay time. If the $^1O_2$-decay time at the place of origin is very long compared to the diffusion time, then nearly all generated $^1O_2$ molecules reach the water phase and the signal component coming from the water phase is nearly not affected.

Therefore the signal amplitude, shown in Figure 5 (C) was determined by the double exponential component only. The additional mono exponential component that can be observed for short delay times (**Figure S9**) after mixing of the *m*-THPC loaded bioconjugates with BSA is neglected as it is

just due to the higher radiative rate constant in aggregates (e.g. micelles), that are progressively decomposed with time in the presence of BSA.

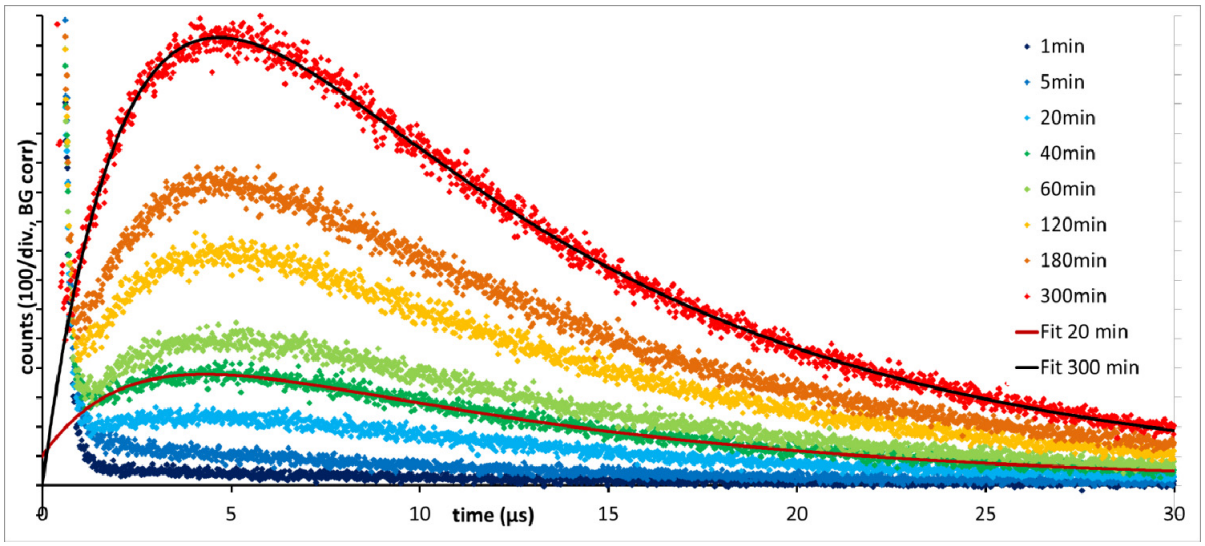

Fig S9. Representative $^1O_2$ luminescence signals determined after mixing of m-THPC/P III with BSA and two fits. While after 20 minutes there is still a mono-exponential component visible and so the fit does not cross the origin, at later stages, the signal can be perfectly fitted by a normal double exponential curve.

Fluorescence anisotropy. Rotation correlation times of the assemblies that were formed after mixing of *m*-THPC loaded bioconjugates with BSA were calculated from polarized time resolved fluorescence measurements parallel and perpendicular to the polarization of the excitation pulse using the equipment described in [11]. The main components of the setup are a thermoelectrically cooled micro channel plate (R3809-01, Hamamatsu), a monochromator (77200, LOT-Oriel) and a PCI TCSPC controller card (SPC630, Becker & Hickl). Excitation wavelength was λ_{exc}=652 nm, fluorescence was recorded at 670 nm.

References

[1] a) J. Sadowski, J. Gasteiger, G. Klebe, *J. Chem. Inf. Comput. Sci.* **1994**, *34*, 1000–1008. b) The 3D structure generator CORINA is available from Molecular Networks GmbH, Erlangen, Germany (http://www.molecular-networks.com).

[2] P.R. Gerber, K. Müller, *J. Comput.-Aided Mol. Des.* **1995**, *9*, 251-268.

[3] LeadIT: LeadIT (version 2.0.2), BioSolveIT GmbH, Sankt Augustin. http://www.biosolveit.de; HYDE: a) I. Reulecke, G. Lange, J. Albrecht, R. Klein, M. Rarey, *ChemMedChem* **2008**, *3*, 885-897. b) N. Schneider, S. Hindle, G. Lange, R. Klein, J. Albrecht, H. Briem, K. Beyer, H. Claußen, M. Gastreich, C. Lemmen, R. Rarey, *J. Comput.-Aided Mol. Des.* **2012**, *23*, 869–881; PYMOL: The PyMOL Molecular Graphics System, Version 1.3, Schrödinger, LLC.

[4] G. Neudert, G. Klebe, *Bioinformatics* **2011**, *27*, 1021–1022.

[5] H. Schnablegger, O. Glatter, *Appl. Opt.* **1991**, *30*, 4889.

[6] J. Schlothauer, S. Hackbarth, B. Röder, *Laser Phys. Lett.* **2009**, *6*, 216.

[7] J. Baier, M. Maier, R. Engl, M. Landthaler, W. Bäumler, *J. Phys. Chem. B.* **2005**, *109*, 3041.

[8] A. Jiménez-Banzo, M.L. Sagristà, M. Mora, S. Nonell, *Free Radical Bio. Med.* **2008**, *44*, 1926.

[9] M.T. Jarvi, M.J. Niedre, M.S. Patterson, B.C. Wilson, *Photochem. Photobiol.* **2011**, *87*, 223.

[10] J.W. Snyder, E. Skovsen, J.D.C. Lambert, P.R. Ogilby PR, *J. Am. Chem. Soc.* **2005**, *127*, 14558.

[11] S. Hackbarth, J. Schlothauer, A. Preuß, B. Röder, *J. Photochem. Photobiol B-Biology* **2010**, *98*, 173.

[12] S. Hackbarth, J. Schlothauer, A. Preuß, C. Ludwig, B. Röder, *Laser Phys. Lett.* **2012**, *9*, 474-480.

[13] S. Makarov, C. Litwinski, E. A. Ermilov, O. Suvorova, B. Röder and D. Wöhrle, *Chem. Eur. J.* **2006**, *12*, 1468-1474.